PCCP

Cite this: *Phys. Chem. Chem. Phys.*, 2012, **14**, 12457–12464

www.rsc.org/pccp

PAPER

Cisplatin cytotoxicity: a theoretical study of induced mutations†

José P. Cerón-Carrasco,[a] Denis Jacquemin*[a] and Emilie Cauët[b]

Received 20th February 2012, Accepted 22nd March 2012
DOI: 10.1039/c2cp40515f

We investigate possible mutations in the genetic code induced by cisplatin with an approach combining molecular dynamics (MD) and hybrid quantum mechanics/molecular mechanics (QM/MM) calculations. Specifically, the impact of platination on the natural tautomeric equilibrium in guanine–cytosine (GC) base pairs is assessed to disclose the possible role played by non-canonical forms in anti-tumour activity. To obtain valuable predictions, the main interactions present in a real DNA environment, namely hydration and stacking, are simultaneously taken into account. According to our results, the Pt–DNA adduct promotes a single proton transfer reaction in GC in the DNA sequence AGGC. Such rare tautomers might play an important role in the cisplatin biological activity since they meet the stability requirements necessary to promote a permanent mutation.

1 Introduction

Since Rosenberg unexpectedly discovered the inhibition of cell division by platinum salts more than forty years ago,[1] Pt complexes have been proposed as anti-tumour agents, and cisplatin has been one of the most widely used drugs in the treatment of cancer.[2] Unfortunately, the clinical use of cisplatin has critical side effects such as neurotoxicity, ototoxicity, tumour resistance and a low solubility in aqueous solution, which eventually limit the tolerable amount and, subsequently, its efficiency.[3]

To circumvent such major drawbacks, huge efforts have been devoted to understand the impact of platinum complexes and to synthesise improved drugs (see for instance the review by Kelland[4] and references therein). Despite its molecular simplicity, the biochemical activity of cisplatin has not yet been fully clarified in part due to the complexity of the real biological environment.[5] Indeed, many cellular components can react with platinum atoms including RNA, proteins, or membrane phospholipids,[6] though it is nowadays accepted that binding to DNA is the ultimate step in the anti-tumour activity.[7] As shown in Fig. 1, the hydrolysis of cisplatin, driven by the lower concentration of Cl^- inside the cellular environment, initially leads to an activated *aqua* complex.[8] This complex subsequently reacts with two adjacent guanine–cytosine base pairs (GC) at N7 sites to predominantly yield the intrastrand Pt–DNA cross-links adduct.[9,10] Consequently, the natural hydrogen bonding and stacking pattern of the double helix is disrupted and the resulting damaged DNA might lead to the programmed cancer cell death,[11] though of course, the complete picture of anti-tumour activity is much more complex than the (over)-simplified Fig. 1.

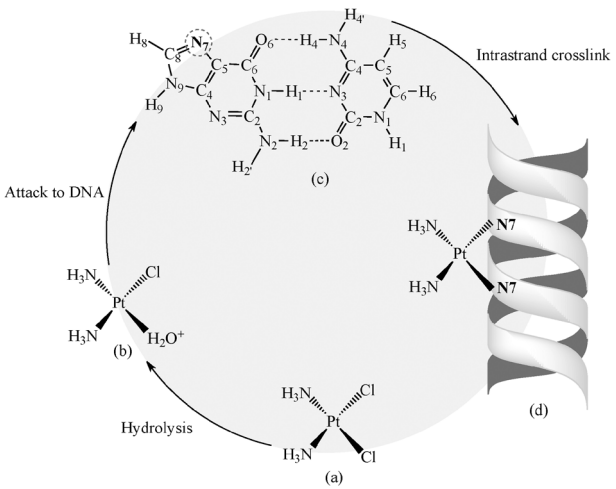

Fig. 1 Main reactions involved in the biochemical activity of cisplatin. Once cisplatin (a) has entered the cell, one water molecule is incorporated into the complex with displacement of one chlorine. The resulting activated *aqua* platinum complex (b) attacks the N7 positions of two adjacent GC base pairs (c) to form the Pt–DNA intrastrand cross-link adduct (d).

From a theoretical point of view, the cisplatin electronic structure and reactivity have been widely investigated to complement experimental data.[12] Most works have been performed in the density functional theory (DFT) framework,[13–21] that provides a valuable balance between accuracy and computational requirements. For instance, Russo and his co-workers have recently demonstrated, with explicit solvent

[a] *CEISAM, UMR CNRS 6230, BP 92208, Université de Nantes, 2, Rue de la Houssinière, 44322 Nantes, Cedex 3, France. E-mail: denis.jacquemin@univ-nantes.fr; Fax: +33 (0)2 5112 5567; Tel: +33 (0)2 5112 5564*
[b] *Service de Chimie Quantique et Photophysique, Université Libre de Bruxelles, 50 Avenue F. D. Roosevelt, B-1050 Bruxelles, Belgium*

† Electronic supplementary information (ESI) available: (1) Cartesian coordinates of the optimised high level layers; (2) atomic charges used during the MD simulations. See DOI: 10.1039/c2cp40515f

models, that hydrolysis of cisplatin is a key activation step before it reaches DNA.[22–25] Another important aspect is the selectivity of cisplatin: it should attack DNA rather than react with other biomolecules such as proteins. Indeed, such side reactions presumably explain the high cisplatin nephrotoxicity.[3] Theoretical calculations confirm that the N7 center is the most reactive position for DNA metallation as discussed by Burda *et al.*,[26–28] who also explored the cisplatin affinity towards sulfur donors present in proteins.[29,30] Most of these *ab initio* studies considered relatively small if not minimal cisplatin–DNA fragments, *e.g.* one or two base pairs, because it is difficult to apply larger models with DFT methods. Alternatively one can go for the hybrid ONIOM approach[31] that combines different methods allowing the investigation of larger (and more realistic) DNA models.[32,33] For instance, Platts and co-workers have used quantum mechanics/molecular mechanics (QM/MM) partition to investigate the structures and binding energies of platinum complexes on single- and double-stranded fragments of DNA.[34,35] They conclude that a cisplatin–DNA complex alters drastically the natural π-stacking between the bases bound to the metal.[34] Besides global DNA changes, ONIOM calculations have also been used to model cisplatin local effects. In particular, Hirao and co-workers[36,37] and Sarmah and Deka[38] have investigated the stability and structure of base pairs covalently bonded to the platinum center. According to these previous investigations, cisplatin could promote the formation of so-called rare tautomers in DNA, that is, non-canonical structures arising from exchanging protons with respect to the original canonical structure. Such proton transfer (PT) reactions are energetically unfavourable in natural DNA,[39–44] but metallation at N7(G) might activate the transfer of the H1 proton in the GC base pair[45–48] and may consequently lead to permanent genetic errors.[49] However, several questions remain unresolved to reach a full understanding of the possible interplay between rare tautomers and cisplatin cytotoxicity. Specifically, previous theoretical works focused on cisplatin did not attempt to estimate the role of water molecules in the PT reactions,[36,37] though they may act as a catalyst for the tautomeric reactions.[50] In addition, the relative energies of the promoted rare tautomers have been computed through single point energy calculations in a two base pair fragment,[36] and consequently the effects of base pair stacking were omitted in these predictions. Finally, there is no information about the lifetime of induced rare tautomers in the biological environment, which is crucial to unravel the impact of metals on the tautomeric equilibria in DNA.[51] This is a key parameter because the adverse effects of metallation at N7(G) might be partially, if not completely, mitigated if the induced PT in the base pair has a low back-reaction barrier allowing a quick return to the canonical form.[51] To gain further insights into this possible cisplatin cytotoxicity mechanism, we address all these issues in the present contribution, which is divided as follows: in Section 2 we design the cisplatin–DNA models and detail our calculation protocol. In Section 3 we present the structures and relative energies along the induced PT reaction. Finally, in Section 4 we interpret our results in terms of biological consequences.

2 Models and theoretical methods

To correctly describe the main interactions in DNA, our model consists of a four base pair model, including the two GC pairs binding cisplatin, the two border base pairs and the lateral sugar–phosphate backbone (Fig. 2). This is the minimal DNA fragment where the π-stacking effects on the base pairs covalently bonded to cisplatin are taken into account. The selected model is based on the structure of the 5′-d(CCTCAGGCCTCC)-3′ dodecamer duplex recently determined by Wu and co-workers with NMR measurements.[52] The underlined letters indicate the guanine bases linked to cisplatin. This DNA fragment was chosen because of the larger cisplatin mutagenic effects in the AGG context compared to CGG, TGG or GGG,[52] which suggests a significant influence of the DNA sequence on the cisplatin activity. Unfortunately, the experimental data do not contain information about the position of the water molecules. Accordingly, we propose an alternative strategy where the experimental cisplatin–DNA dodecamer is embedded into a cubic box of water to perform molecular dynamics (MD) simulations. The resulting equilibrated system has subsequently been used for the design of a new four base pair model surrounded by the first hydration shell. The explicit solvent model was used to determine the role of water molecules in PT reactions. Additionally, the MD calculations provided further evidence about the conformation adopted by the cisplatin–DNA adduct in an aqueous environment.

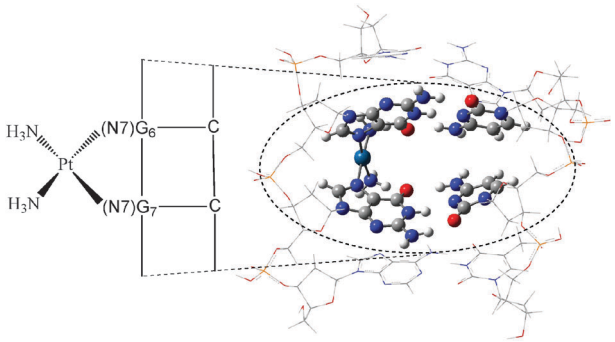

Fig. 2 Four base pair model for ONIOM calculations: the cisplatin and the two binding GC base pairs (G_6C and G_7C) to the Pt atom, corresponding to the high level layer, are represented with balls and sticks. The border base pairs and lateral backbone, included in the low layer, are displayed in wireframe.

2.1 ONIOM calculations

We have tested several theoretical levels to ascertain the quality of our chemical conclusions. The starting geometry for these ONIOM benchmarks is the cisplatin–DNA high-resolution NMR solution structure as deposited in the Protein Data Bank by Wu *et al.* (PDB: 2NPW).[52] The cisplatin complex and the two GC pairs covalently linked to Pt are selected as the high layer, hereafter denoted simply $(G_6C)Pt(G_7C)$. The subscript numbers refer to the base pair position in the experimental DNA dodecamer with a 5′-d(CCTCAGGCCTCC)-3′ sequence. The border base pairs confining the high layer and the backbone structure (sugar and phosphate moieties) are located in the low layer. At this stage phosphate groups are protonated, since they have a limited impact on the tautomeric equilibrium in DNA.[51,53] The resulting four base pair model is shown in Fig. 2. As listed in Table 1, several ONIOM approaches have been tested. The high layer atoms were fully optimised with the

M06-2X functional,[54,55] which has been shown to be very effective for biomolecules,[56–63] and the 6-311++G(d,p) atomic basis set on H, C, N, and O atoms (Lanl2DZ basis set and pseudopotential for platinum). For the low layer the Universal Force Field (UFF)[64] has been applied. Let us clarify the QM/MM approach used in the present work by discussing briefly the ONIOM methodology as implemented in Gaussian09.[65] In a two layer ONIOM approach the energy of a given system is expressed as

$$E(\text{ONIOM}) = E_{\text{real}}(\text{MM}) + E_{\text{model}}(\text{QM}) - E_{\text{model}}(\text{MM}) \quad (1)$$

where the subscripts refer to the real system (containing all the atoms) and to the model (high layer), whereas the labels between brackets indicate the theoretical level of calculation. Consequently, within this formalism the coupling between the QM and MM regions is solely described at the MM level, a procedure known as mechanical embedding (ME).[66] This simple approximation provides a reasonable approach to both steric effects and weak interactions, but might be problematic for the description of electrostatic interactions.[67] This shortcoming can be partially circumvented by incorporating the partial MM charges in an additional term of the QM Hamiltonian, a procedure referred to as electronic embedding (EE).[68] These mechanical and electronic embedding schemes have been used to assess the impact of the electronic coupling in the final PT energetic profile as listed in Table 1. Aiming to reach a tractable model, and taking into account that relaxation of lateral sugar–phosphate backbones and border bases is expected to have a minor influence on the PT reactions,[36,53,69] atoms in the low layer are frozen in space, subsequently allowing us to use an accurate high layer method. Although the vibrational calculations with a frozen low layer should be analysed cautiously, the absence of imaginary frequencies (for a minimum), and the presence of a single imaginary mode related to the N1(G)–H1–N3(C) stretching (transition state) confirm the nature of the structures (see Fig. 1 for atomic numbering).

Finally we discuss the models used to treat the solvent effects, which are known to tune both metal bonding and GC tautomeric equilibrium.[70–73] As depicted in Table 1, the well-known polarisable continuum model (PCM)[74] is included following (i) single point energy calculations performed on the gas phase geometries, and (ii) optimisations in condensed phase. Testing all these protocols allowed us to select the "best compromise" method to explore the role of explicit water molecules in the PT process in a later step. To this end, an explicit solvent model has been designed through MD simulations (see the next section). In this model, the ONIOM model is based on the equilibrated cisplatin–DNA complex structure following the ONIOM partition scheme. The comparisons between gas phase, PCM and PCM + explicit solvent models allowed us to investigate the role of water molecules in the cisplatin-induced tautomerism.

Table 1 Theoretical methods for the description of the low layer within the two-layer ONIOM approach

Method	Calculation	Low layer	PCM	MM[a]
1	Optimisation	UFF		ME
2	Single point[b]	UFF	✓	ME
3	Single point[b]	UFF	✓	EE
4	Optimisation	UFF	✓	EE

[a] Molecular (ME) or electronic (EE) embedding schemes. [b] SP calculation on the geometry optimised with method 1.

2.2 MD simulations

To search a large conformational space and provide information on the dynamics and position of water molecules surrounding the cisplatin-adducted DNA model, MD simulations were performed with the NWChem program package.[75] The starting structure used is the cisplatin–DNA dodecamer structure as described in the previous section. Sodium counterions were added so as to counterbalance the total charge of the complex. This complex was immersed in a periodic 60 Å cubic box filled with water molecules, at a density of 1.0 g cm^{-3}. The final number of water molecules is 6847. The initial structure was first relaxed by short steepest descent minimisation runs of 1000 steps. The structural model underwent then an equilibration phase *via* classical MD, carried out using the AMBER force field[76] for both DNA and sodium counterions. For the cisplatin adduct and the guanine bases G6 and G7, the parametrization of Scheeff *et al.* was used.[77] The partial charges for the cisplatin adduct and the two bound guanines were, however, adapted based on *ab initio* calculations that we performed on the system with the M06-2X functional and the same basis set used above. The Mulliken approach[78] has been employed for localising the charges in the cluster. The resultant charges are provided in ESI.† The solvent water molecules were treated with the SPC/E model.[79] Electrostatics were evaluated with the Particle Mesh Ewald (PME) method.[80,81] A time step of 1 fs was applied. Room temperature simulations were achieved by coupling the system to a Berendsen thermostat.[82] 60 ps MD simulation at constant volume was performed during which the system was heated in stages up to 298.15 K. 200 ps MD simulation at constant pressure (1 atm) and temperature (298.15 K) was then performed. Because significant base pair-opening events were observed during the dynamics, we decided, as done by Scheeff *et al.*, to constrain the simulation by fixing the position of the terminal phosphorous atoms at the 5′ and 3′-ends of both strands. Although this arrangement reduced the size of the conformational space, it was sufficient to prevent base opening and provided protection against degradation of the overall structure of the molecule.

3 Results and discussion

3.1 Benchmarks

We start by analysing the results obtained with the ONIOM partition when using the experimental NMR cisplatin–DNA structure as starting point, that is, with no intermediate MD equilibration nor explicit water molecules. As shown in Table 1, different methods have been designed to assess the impact of the molecular mechanic scheme (ME and EE) as well as the PCM corrections on the PT reactions. According to the computed potential energy curves along the H1 transfer (Fig. 3) the theoretical approach could significantly affect the

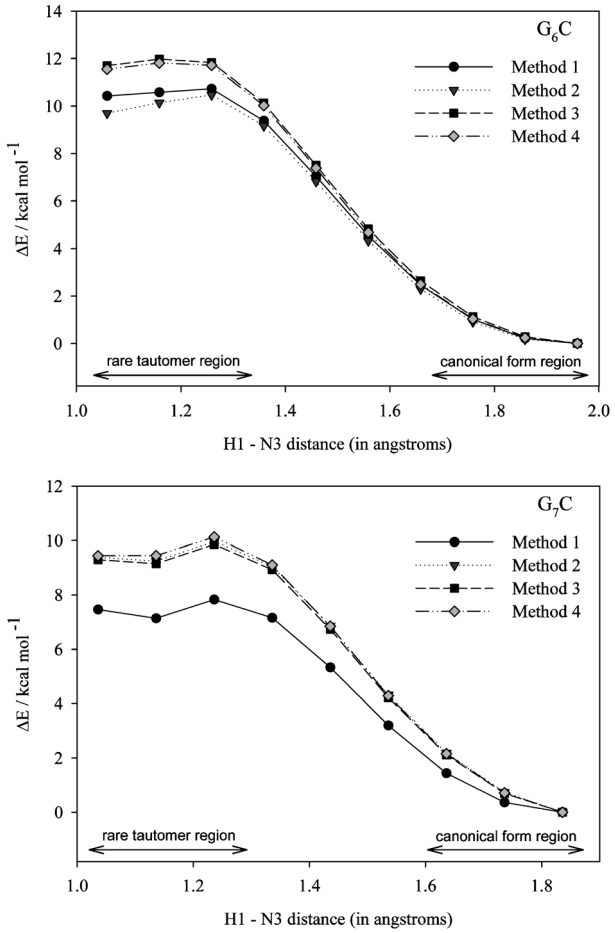

Fig. 3 Energy profiles along with the H1 proton transfer in G_6C (above) and G_7C (below) base pairs. All geometrical parameters (except the scanning H1–N3 bond distance) are relaxed. The relative electronic energies are given with respect to the canonical form.

predicted rare tautomers stability. Indeed, the comparison of the simplest method (1) and of the most elaborated approach (4) shows that the inclusion of both EE and PCM during the optimisation induces a destabilisation of *ca.* 2 kcal mol^{-1} of the rare tautomeric structure, which proves the importance of both electrostatic interactions and dielectric effects. Furthermore, method 3 provides very similar results to method 4, which clearly indicates that EE and PCM corrections can be obtained through single point calculations on the geometry of method 1. In contrast, method 2 only provides a similar trend as method 4 for G_7C, whereas a sizeable energy difference is found for the G_6C base pairs. Consequently, to ensure consistent results for both base pairs, PCM corrections should be carried out within the EE scheme.

Inspection of Fig. 3 also reveals that the H1 proton transfer follows different energetic profiles for the two Pt-bonded base pairs. This dissimilarity can be analysed in terms of two variables, namely the different conformations adopted by the base pairs and the DNA sequence. More precisely, the optimised structures (both methods 1 and 4) reveal a larger distortion of planarity for G_6C than for G_7C as a result of the cisplatin binding to DNA. Since the coplanarity of the atoms involved in PT is a key parameter,[83,84] the planarity of the GC base pair has been described in terms of the absolute value of the C6(G)C2(G)C2(C)C4(C) dihedral angle (see Fig. 1 for atomic numbering). This angle lies around 13° and 7° for the rare tautomeric forms of G_6C and G_7C base pairs, respectively (method 1). Additionally, there are different chemical environments around the cisplatin binding base pairs in the selected AGGC sequence, as discussed above.

Table 2 Relative electronic energies (ΔE/kcal mol^{-1}) computed along H1 proton transfer in the G_6C and G_7C base pairs taking the canonical structure as reference. The method refers to the schemes listed in Table 1

	G_6C		G_7C	
Method	TS	Rare tautomer	TS	Rare tautomer
1	10.98	10.24	7.32	6.88
2	10.57	9.48	8.98	8.87
3	12.06	11.56	8.99	8.78
4	11.89	11.33	9.29	9.06

Once the critical points on the energy profiles along PT reactions have been identified as canonical, transition state (TS) and rare tautomeric forms, the high layer has been fully optimised (without any restriction on the H1–N3 distance). The predicted energies are collected in Table 2. According to the more refined ONIOM approaches (methods 3 and 4) the relative energy of the rare tautomers is in the range of 9–12 kcal mol^{-1} above the canonical structure. Interestingly, data in Table 2 suggest that the rare tautomeric forms are practically isoenergetic with the TS connecting them to the canonical structure, a conclusion holding both in gas phase and under the influence of the dielectric continuum. This is in agreement with the very shallow minima identified during the scan (Fig. 3) and the very small backward energy barrier to the canonical structure (<1 kcal mol^{-1}). Accordingly, within this first model the tautomeric forms are expected to have very short lifetimes hinting that the impact of rare tautomers on cisplatin cytotoxicity could be negligible. Indeed, as Florián and Leszczyński discussed a rare tautomer structure could lead to a mutation only if the energetic barrier for the reverse PT is larger than about 3 kcal mol^{-1},[39] and the cisplatin-induced rare tautomers are clearly far from satisfying this requirement. We have also explored the stability of the putative rare tautomer resulting from simultaneous PT reactions in both G_6C and G_7C base pairs. As expected it is not possible to localise a minimum corresponding to this configuration. This outcome can be explained: the PT reactions in GC base pairs lead to a negatively charged guanine and positively charged cytosine.[36,38] Hence, the simultaneous PT reactions in two contiguous GC base pairs, G_6C and G_7C, imply strong repulsions. Eventually, we looked for double proton transfer (DPT) reactions, in which one of the GC base pairs exchanges both the H1 and H4 protons (see Fig. 2), but no stable DPT product could be isolated. This is an expected result since we have recently demonstrated the inaccessibility of the DPT mechanism in metallated GC derivates.[51]

It is notable that our results partially differ from those reported in the pioneering study by Hirao and co-workers,[36] who located the Pt-induced rare tautomers at *ca.* 3 kcal mol^{-1} above the canonical structure. However, we should point out that several factors prevent an equal footing comparison of the

values in Table 2 with these earlier data since (i) in Hirao's work the high layer was "extracted" before computing the relative stability of rare tautomers whereas Table 2 lists the ONIOM energies, including all interactions between QM and MM regions; (ii) the selected theoretical levels are not coincident because those previously reported energies are computed with a smaller basis set and a less "modern" functional (mPW1PW91/6-31G(d,p)) than in the present paper; (iii) the DNA structures also differ, Hirao and coworkers considered a TGG sequence but as noted above we used a fragment where cisplatin is binding to DNA in a more mutagenic AGG sequence;[36,52] and (iv) in Hirao's study the four base pair model is fully optimised without any restriction[36] whereas, in our model, the atomic positions of the border base pairs and lateral sugar–phosphate backbone, located in the low layer, are frozen. The former procedure presents the advantage of computing the full Hessian, yielding a true (mathematical) minimum. However, the flexibility of the base pairs is much larger in a short DNA sequence than under real biological conditions, where not only vicinal but also further DNA regions restrict the geometrical flexibility of the $(G_6C)Pt(G_7C)$ entity. Consequently, the full optimisation of relatively small models as the one shown in Fig. 2 could lead to an over-distorted structure. In this framework, aiming to improve our model by ascertaining the DNA deformation, MD simulations have been carried out on the hydrated cisplatin–DNA dodecamer molecule rather than by performing full optimisation of the four base pair fragment.

3.2 Equilibrated cisplatin–DNA

It can be inferred from the discussion in the previous section that stacking impacts the PT process and therefore border base pairs confining the $(G_6C)Pt(G_7C)$ moiety should be adequately accounted for characterising the influence of cisplatin on DNA structure. Furthermore, since water molecules might be involved in the PT process[73,85] an explicit solvent model might be necessary to mimic the aqueous environment in which biological DNA is found. Accordingly, MD calculations have been carried out to determine both the conformation of cisplatin–DNA in solution and the hydrated pattern around the base pairs involved in the PT process. The starting geometry for MD simulations is the same experimental cisplatin–DNA structure as the one used during our ONIOM benchmark.[52] Since we select as the starting point the experimental NMR structure one might expect that the MD calculations lead to a very similar structure as the equilibration is performed in a water box. However, as illustrated in Fig. 4 it is obvious that base pairs depart from planarity during the equilibration process. To analyse the origin of such discrepancy let us briefly describe the effective experimental approaches. Most of the available cisplatin–DNA NMR structures have been determined with the same protocol, which includes the synthesis and purification of the selected oligonucleotide followed by the treatment with activated cisplatin.[86,87] The resulting cisplatin–oligonucleotide adduct is subsequently characterised by several techniques, *e.g.* liquid chromatography or mass spectroscopy, prior to the NMR experiments in D_2O. Unfortunately, it is not possible to define a single structural model exclusively from experimental evidence due to the huge complexity of the system, and the

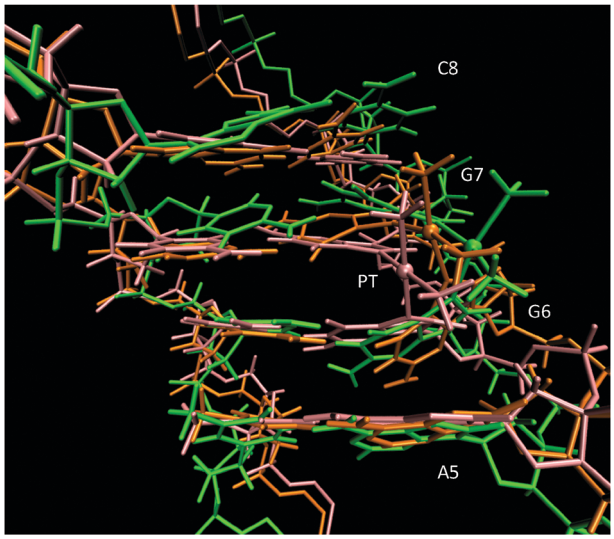

Fig. 4 Stereoviews of the equilibrated structures at 10 (orange), 100 (blue) and 200 (green) ps, respectively. For the sake of clarity water molecules are not shown. A5, G6, G7 and C8 refer to the position of the adenine, guanine, cytosine bases, respectively, in the 5′-d(CCTCAGGCCTCC)-3′ sequence.

final structure needs to be refined by means of restrained-MD calculations, where several structural constraints are imposed to fit the experimental data. In the particular case of the 2NPW pdb structure, the final atomic positions have been estimated by imposing constraints in the NMR-derived distances as well as enforcing planarity for all base pairs other than the two directly bonded to cisplatin, namely G_6C and G_7C.[52] In contrast, only terminal phosphorous atoms position constraints have been used in our calculations to ensure the stability of the double helix structure. Consequently, the evolution of the geometry shown in Fig. 4 is the logical consequence of relaxing the internal tensions in the over-constrained initial NMR structure.

To investigate how these changes affect the tautomeric processes, the equilibrated geometry at 200 ps is chosen to define a suitable model for ONIOM calculations (method 3 of Table 1). First, the same pattern as the one used in the benchmark calculations is selected from the final snapshot of classical MD simulations: the $(G_6C)Pt(G_7C)$ moiety is in the high layer whereas the border base pairs and the backbone structure are placed in the low layer. As previously described, atoms in the high layer are fully optimised while those in the low layer are frozen in space. The relative PT energies of this structure, defined as model A, are listed in Table 3. A comparison between Tables 2 and 3 indicates that DNA MD relaxation has only a minor effect (less than 1 kcal mol^{-1}) on the PT reaction in the G_7C base pair. Accordingly, the rare tautomer of that base pair has only a trifling macroscopic effect in DNA due to its short lifetime (TS too close to the product). On the other hand, a larger change is predicted for the PT energetic profile of the G_6C base pair with a significant stabilisation (*ca.* 5 kcal mol^{-1}) of the rare tautomer, but only a minor variation of the TS energy. Subsequently, the induced G_6C rare tautomer satisfies the criteria to promote a permanent error in the genetic code (reverse PT barrier exceeds 3 kcal mol^{-1}).[39] This is a remarkable result: cisplatin induces a rare tautomeric

Table 3 Relative electronic energies (ΔE/kcal mol^{-1}) computed along H1 proton transfer in the G_6C and G_7C base pairs on the MD equilibrated cisplatin–DNA geometry. The canonical structure is considered as reference

	G_6C		G_7C	
Model[a]	TS	Rare tautomer	TS	Rare tautomer
A	12.48	6.70	9.97	8.31
B	13.13	7.03	12.25	11.93

[a] In the absence (A) or presence (B) of explicit water molecules.

form only in one of the GC base pairs covalently binding to the metal. As noted in Section 3.1, the energetic profiles for PT in G_6C and G_7C are not coincident because of the dissimilar planarity of the base pairs as well as the different chemical environment. Since the planarity of the system facilitates PT reactions through hydrogen bonds,[83,84] let us compare the $(G_6C)Pt(G_7C)$ moiety obtained using the experimental NMR data and the MD equilibration technique to explain the stabilisation of the G_6C rare tautomer. As discussed above, ONIOM calculations on the NMR structure yield C6(G)C2(G)C2(C)C4(C) dihedral angles around 13° and 7° for the rare tautomeric forms of G_6C and G_7C base pairs, respectively, which are consistent with the relative energies of 11.56 and 8.78 kcal mol^{-1} (see Table 2, method 3). In contrast, when the MD equilibrated structure is selected as the starting point, the optimised structures of the rare tautomeric forms of G_6C and G_7C base pairs deviate from planarity by only 1° and 6°, respectively. Hence, the stabilisation of the G_6C rare tautomer could be rationalised by the enhancement of its planarity resulting from equilibration.

To completely characterise the cisplatin-induced PT mechanism in DNA, a micro-hydrated model has been also designed. Specifically, we have added 3 Å radius spheres on all the hetero-atoms of G_6C and G_7C of the equilibrated cisplatin–DNA structure to locate the key water molecules in the first hydration shell. Eight water molecules have been found and were incorporated in the high (QM) layer together with the $(G_6C)Pt(G_7C)$ moiety to simulate the specific solvent effects. The border base pairs confining the high layer and the backbone structure are placed in the low layer. The resulting system, defined as model B (Fig. 5), is optimised in its canonical form as previously: the high layer is fully relaxed while the low layer is fixed in space. According to the resulting hydration pattern, water molecules cannot act as a catalyst of the DPT process because they are not located at the required positions to assist the H4′ proton transfer from N4(C) to O6(G) atoms (see atomic numbering in Fig. 1). This is consistent with our model because, contrary to the free-metal GC base pair where the O6(G) site is complexed by surrounding water molecules,[88] that position is occupied by the ammonia ligand in the cisplatin–DNA adduct. This confirms the inaccessibility of the DPT mechanism neither through a direct nor water-assisted mechanism and contrasts with the Grotthus-like mechanism that takes place in natural DNA.[50] Since water molecules affect the cisplatin–DNA conformation but do not play an active role in the PT reactions, it is expected that they remain unchanged during the H1 proton transfer.[89] Accordingly, in model B the explicit water molecules are fixed during the optimisation of the rare tautomeric forms. The predicted energies listed in Table 3 reveal a destabilisation of the G_7C base pair and only a minor impact in the G_6C base pair. These results back up the proposed relative stability along the cisplatin-induced tautomerism in DNA and confirm the G_6C rare tautomer as a well-suited candidate to promote the observed *in vivo* cisplatin cytotoxicity.

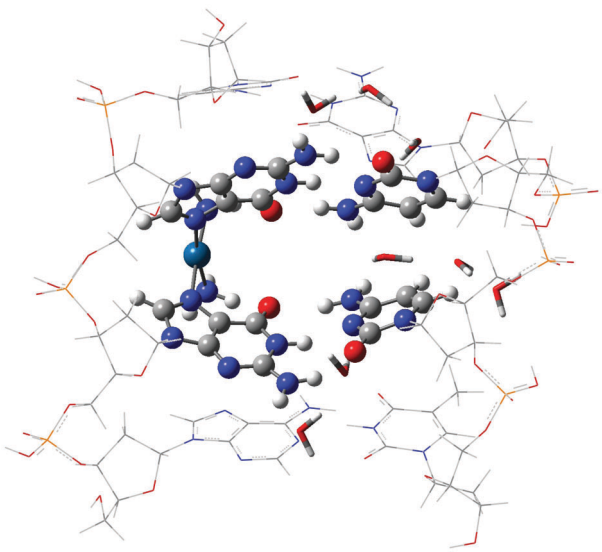

Fig. 5 Model B: the cisplatin and the two binding GC base pairs (G_6C and G_7C) to the Pt atom are represented with balls and sticks while the eight water molecules corresponding to the first hydration shell are shown in a tube. All these atoms are placed in the high level layer of the ONIOM partition.

4 Conclusions and outlook

We have studied the influence of cisplatin on DNA structure by state-of-the-art theoretical tools. The comparison of two selected DNA models (the one designed directly from NMR solution structures and its counterpart resulting from MD calculations) allowed us to evaluate not only the interplay between the environment and the geometries of the base pairs but also the influence of π-stacking on the rare tautomer stability. According to our calculations, the permanent mutation arising from a proton transfer reaction can only be found when the cisplatin–DNA system has been equilibrated. This result highlights the energetic consequences of the severe DNA distortion resulting from the constraints used during NMR analysis. Consequently, while in metal-free DNA systems (where the planarity of the base pairs is not perturbed) the experimental data represent a reasonable starting point for QM/MM simulations, in cisplatin–DNA derivatives (where the π-stacking is disrupted) a previous MD equilibration might be necessary. Although the role played by the actual DNA sequence is certainly much more complex than a pure "steric" interaction, our results confirm that the planarity of the rare tautomeric forms is probably a non-negligible factor for estimating the possibility of mutagenic proton transfer. In the present study, we found that part of the cisplatin action is to promote the apparition of relatively stable rare tautomers in the most planar GC base pair directly bonded to cisplatin.

Acknowledgements

J.P.C.C. acknowledges the fellowship provided by the Fundación Séneca, Agencia de Ciencia y Tecnología de la Región de Murcia, within its Postdoctoral Research Staff Training Program. D.J. acknowledges the European Research Council (ERC) and the *Région des Pays de la Loire* for financial support in the framework of Starting Grant (Marches - 278845) and a *recrutement sur poste stratégique*, respectively. E.C. thanks the F.R.S.-FNRS (Fonds National de la Recherche Scientifique de Belgique) and the Communauté Française de Belgique (ARC contract). This research used resources of the GENCI-CINES/IDRIS (Grants c2011085117 and c2012085117), and of the CCIPL (*Centre de Calcul Intensif des Pays de Loire*).

References

1 B. Rosenberg, L. VanCamp and T. Krigas, *Nature*, 1965, **205**, 698–699.
2 Y. Jung and S. J. Lippard, *Chem. Rev.*, 2007, **107**, 1387–1407.
3 E. Wong and C. M. Giandomenico, *Chem. Rev.*, 1999, **99**, 2351–2466.
4 L. Kelland, *Nat. Rev. Cancer*, 2007, **7**, 573–584.
5 V. M. Gonzalez, M. A. Fuertes, C. Alonso and J. M. Pérez, *Mol. Pharmacol.*, 2001, **59**, 657–663.
6 E. R. Jamieson and S. J. Lippard, *Chem. Rev.*, 1999, **99**, 2467–2498.
7 V. Cepeda, M. A. Fuertes, J. Castilla, C. Alonso, C. Quevedo and J. M. Pérez, *Anticancer Agents Med. Chem.*, 2007, **7**, 3–18.
8 J. K.-C. Lau and B. Ensing, *Phys. Chem. Chem. Phys.*, 2010, **12**, 10348–10355.
9 R. P. Pérez, *Eur. J. Cancer*, 1998, **34**, 1535–1544.
10 J. Reedijk, *Chem. Rev.*, 1999, **99**, 2499–2510.
11 M. A. Fuertes, C. Alonso and J. M. Pérez, *Chem. Rev.*, 2003, **103**, 645–662.
12 Y. Mantri and M.-H. Baik, in *Computational Studies: Cisplatin*, John Wiley & Sons, Ltd, 2006.
13 J. V. Burda, J. Šponer and J. Leszczyński, *JBIC, J. Biol. Inorg. Chem.*, 2000, **5**, 178–188.
14 Y. Zhang, Z. Guo and X.-Z. You, *J. Am. Chem. Soc.*, 2001, **123**, 9378–9387.
15 M.-H. Baik, R. A. Friesner and S. J. Lippard, *J. Am. Chem. Soc.*, 2003, **125**, 14082–14092.
16 M. Zeizinger, J. V. Burda and J. Leszczyński, *Phys. Chem. Chem. Phys.*, 2004, **6**, 3585–3590.
17 A. Robertazzi and J. A. Platts, *Inorg. Chem.*, 2005, **44**, 267–274.
18 D. V. Deubel, *J. Am. Chem. Soc.*, 2006, **128**, 1654–1663.
19 P. Sarmah and R. C. Deka, *Int. J. Quantum Chem.*, 2008, **108**, 1400–1409.
20 A. Melchior, E. S. Marcos, R. R. Pappalardo and J. M. Martínez, *Theor. Chem. Acc.*, 2011, **128**, 627–638.
21 M. E. Alberto, V. Butera and N. Russo, *Inorg. Chem.*, 2011, **50**, 6965–6971.
22 M. Pavelka, M. F. A. Lucas and N. Russo, *Chem.–Eur. J.*, 2007, **13**, 10108–10116.
23 M. F. A. Lucas, M. Pavelka, M. E. Alberto and N. Russo, *J. Phys. Chem. B*, 2009, **113**, 831–838.
24 M. E. Alberto, M. F. A. Lucas, M. Pavelka and N. Russo, *J. Phys. Chem. B*, 2009, **113**, 14473–14479.
25 M. E. Alberto and N. Russo, *Chem. Commun.*, 2011, **47**, 887–889.
26 J. V. Burda, J. Šponer and J. Leszczyński, *Phys. Chem. Chem. Phys.*, 2001, **3**, 4404–4411.
27 J. V. Burda and J. Leszczyński, *Inorg. Chem.*, 2003, **42**, 7162–7172.
28 M. Pavelka and J. V. Burda, *J. Mol. Model*, 2007, **13**, 367–379.
29 T. Zimmermann, Z. Chval and J. V. Burda, *J. Phys. Chem. B*, 2009, **113**, 3139–3150.
30 T. Zimmermann, M. Zeizinger and J. V. Burda, *J. Inorg. Biochem.*, 2005, **99**, 2184–2196.
31 S. Dapprich, I. Komáromi, K. S. Byun, K. Morokuma and M. J. Frisch, *J. Mol. Struct. (THEOCHEM)*, 1999, **462**, 1–21.
32 P. F. Loos, E. Dumont, A. Laurent and X. Assfeld, *Chem. Phys. Lett.*, 2009, **475**, 120–123.
33 D. Ambrosek, P. F. Loos, X. Assfeld and C. Daniel, *J. Inorg. Biochem.*, 2010, **104**, 893–901.
34 A. Robertazzi and J. A. Platts, *Chem.–Eur. J.*, 2006, **12**, 5747–5756.
35 K. Gkionis and J. A. Platts, *JBIC, J. Biol. Inorg. Chem.*, 2009, **14**, 1165–1174.
36 T. Matsui, Y. Shigeta and K. Hirao, *J. Phys. Chem. B*, 2007, **111**, 1176–1181.
37 T. Matsui, Y. Shigeta and K. Hirao, *Chem. Phys. Lett.*, 2006, **423**, 331–334.
38 P. Sarmah and R. C. Deka, *Chem. Phys. Lett.*, 2011, **508**, 295–299.
39 J. Florián and J. Leszczyński, *J. Am. Chem. Soc.*, 1996, **118**, 3010–3017.
40 V. Guallar, A. Douhal, M. Moreno and J. M. Lluch, *J. Phys. Chem. A*, 1999, **103**, 6251–6256.
41 J. J. Dannenberg and M. Tomasz, *J. Am. Chem. Soc.*, 2000, **122**, 2062–2068.
42 L. Gorb, Y. Podolyan, P. Dziekonski, W. A. Sokalski and J. Leszczyński, *J. Am. Chem. Soc.*, 2004, **126**, 10119–10129.
43 J. P. Cerón-Carrasco, A. Requena, C. Michaux, E. A. Perpète and D. Jacquemin, *J. Phys. Chem. A*, 2009, **113**, 7892–7898.
44 G. Villani, *J. Phys. Chem. B*, 2010, **114**, 9653–9662.
45 B. Song, J. Zhao, R. Griesser, C. Meiser, H. Sigel and B. Lippert, *Chem.–Eur. J.*, 1999, **5**, 2374–2387.
46 J. Šponer, M. Sabat, L. Gorb, J. Leszczyński, B. Lippert and P. Hobza, *J. Phys. Chem. B*, 2000, **104**, 7535–7544.
47 M. Noguera, J. Bertran and M. Sodupe, *J. Phys. Chem. A*, 2004, **108**, 333–341.
48 M. Noguera, J. Bertrán and M. Sodupe, *J. Phys. Chem. B*, 2008, **112**, 4817–4825.
49 P. O. Löwding, *Rev. Mod. Phys.*, 1963, **35**, 724–732.
50 J. P. Cerón-Carrasco, J. Zúñiga, A. Requena, E. A. Perpète, C. Michaux and D. Jacquemin, *Phys. Chem. Chem. Phys.*, 2011, **13**, 14584–14589.
51 J. P. Cerón-Carrasco and D. Jacquemin, *ChemPhysChem*, 2011, **12**, 2615–2623.
52 Y. Wu, D. Bhattacharyya, C. L. King, I. Baskerville-Abraham, S.-H. Huh, G. Boysen, J. A. Swenberg, B. Temple, S. L. Campbell and S. G. Chaney, *Biochemistry*, 2007, **46**, 6477–6487.
53 H.-Y. Chen, C.-L. Kao and S. C. N. Hsu, *J. Am. Chem. Soc.*, 2009, **131**, 15930–15938.
54 Y. Zhao, N. E. Schultz and D. G. Truhlar, *Acc. Chem. Res.*, 2008, **41**, 157–167.
55 Y. Zhao and D. G. Truhlar, *Theor. Chem. Acc.*, 2008, **120**, 215–241.
56 E. G. Hohenstein, S. T. Chill and C. D. Sherrill, *J. Chem. Theor. Comput.*, 2008, **4**, 1996–2000.
57 J. Gu, J. Wang, J. Leszczynski, Y. Xie and H. F. Schaefer-III, *Chem. Phys. Lett.*, 2008, **459**, 164–166.
58 A. Bende, *Theor. Chem. Acc.*, 2010, **125**, 253–268.
59 J. C. Hargis, H. F. Schaefer-III, K. N. Houk and S. E. Wheeler, *J. Phys. Chem. A*, 2010, **114**, 2038–2044.
60 M. K. Shukla and J. Leszczyński, *Mol. Phys.*, 2010, **108**, 3131–3146.
61 Y. Paukku and G. Hill, *J. Phys. Chem. A*, 2011, **115**, 4804–4810.
62 A. Kumar and M. D. Sevilla, *J. Phys. Chem. B*, 2011, **115**, 4990–5000.
63 Y. Zhao and D. G. Truhlar, *J. Chem. Theor. Comput.*, 2011, **7**, 669–676.
64 A. K. Rappé, C. J. Casewit, K. S. Colwell, W. A. G. III and W. M. Skiff, *J. Am. Chem. Soc.*, 1992, **114**, 10024–10035.
65 M. J. Frisch, G. W. Trucks, H. B. Schlegel, G. E. Scuseria, M. A. Robb, J. R. Cheeseman, G. Scalmani, V. Barone, B. Mennucci, G. A. Petersson, H. Nakatsuji, M. Caricato, X. Li, H. P. Hratchian, A. F. Izmaylov, J. Bloino, G. Zheng, J. L. Sonnenberg, M. Hada, M. Ehara, K. Toyota, R. Fukuda, J. Hasegawa, M. Ishida, T. Nakajima, Y. Honda, O. Kitao, H. Nakai, T. Vreven, J. A. Montgomery, Jr., J. E. Peralta, F. Ogliaro, M. Bearpark, J. J. Heyd, E. Brothers, K. N. Kudin, V. N. Staroverov, R. Kobayashi, J. Normand, K. Raghavachari, A. Rendell, J. C. Burant, S. S. Iyengar, J. Tomasi, M. Cossi, N. Rega, J. M. Millam, M. Klene, J. E. Knox, J. B. Cross, V. Bakken, C. Adamo, J. Jaramillo, R. Gomperts, R. E. Stratmann, O. Yazyev, A. J. Austin, R. Cammi, C. Pomelli, J. W. Ochterski, R. L. Martin,

K. Morokuma, V. G. Zakrzewski, G. A. Voth, P. Salvador, J. J. Dannenberg, S. Dapprich, A. D. Daniels, Ö. Farkas, J. B. Foresman, J. V. Ortiz, J. Cioslowski and D. J. Fox, *Gaussian 09, Revision A.02*, Gaussian Inc., Wallingford, CT, 2009.
66 H. M. Senn and W. Thiel, *Angew. Chem., Int. Ed.*, 2009, **48**, 1198–1229.
67 C. Bo and F. Maseras, *Dalton Trans.*, 2008, 2911–2919.
68 T. Vreven, K. S. Byun, I. Komáromi, S. Dapprich, J. A. Montgomery, Jr, K. Morokuma and M. J. Frisch, *J. Chem. Theor. Comput.*, 2006, **2**, 815–826.
69 H.-Y. Chen, S.-W. Yeh, S. C. N. Hsu, C.-L. Kao and T.-Y. Dong, *Phys. Chem. Chem. Phys.*, 2011, **13**, 2674–2681.
70 J. Šponer, J. V. Burda, M. Sabat, J. Leszczyński and P. Hobza, *J. Phys. Chem. A*, 1998, **102**, 5951–5957.
71 C. Alemán, *Chem. Phys.*, 1999, **224**, 151–162.
72 C. Alemán, *Chem. Phys.*, 2000, **253**, 13–19.
73 J. P. Cerón-Carrasco, A. Requena, J. Zúñiga, C. Michaux, E. A. Perpète and D. Jacquemin, *J. Phys. Chem. A*, 2009, **113**, 10549–10556.
74 J. Tomasi, B. Mennucci and R. Cammi, *Chem. Rev.*, 2005, **105**, 2999–3093.
75 M. Valiev, E. J. Bylaska, N. Govind, K. Kowalski, T. P. Straatsma, H. J. J. van Dam, D. Wang, J. Nieplocha, E. Apra, T. Windus and W. A. de Jong, *Comput. Phys. Commun.*, 2010, **181**, 1477.
76 W. D. Cornell, P. Cieplak, C. I. Bayly, I. R. Gould, K. M. Merz, D. M. Ferguson, D. C. Spellmeyer, T. Fox, J. W. Caldwell and P. A. Kollman, *J. Am. Chem. Soc.*, 1995, **117**, 5179–5197.
77 E. D. Scheeff, J. M. Briggs and S. B. Howell, *Mol. Pharmacol.*, 1999, **56**, 633–643.
78 R. S. Mulliken, *J. Chem. Phys.*, 1962, **36**, 3428.
79 H. J. C. Berendsen, J. R. Grigera and T. P. Straatsma, *J. Phys. Chem.*, 1987, **91**, 6269–6271.
80 T. A. Darden, D. M. York and L. G. Pedersen, *J. Chem. Phys.*, 1993, **98**, 10089–10092.
81 D. M. York, T. A. Darden and L. G. Pedersen, *J. Chem. Phys.*, 1993, **99**, 8345–8348.
82 H. J. C. Berendsen, J. P. M. Postma, W. F. van Gunsteren, A. DiNola and J. R. Haak, *J. Chem. Phys.*, 1984, **81**, 3684–3690.
83 M. Barbatti, A. J. A. Aquino, H. Lischka, C. Schriever, S. Lochbrunner and E. Riedle, *Phys. Chem. Chem. Phys.*, 2009, **11**, 1406–1415.
84 R. Daengngern, N. Kungwan, P. Wolschann, A. J. A. Aquino, H. Lischka and M. Barbatti, *J. Phys. Chem. A*, 2011, **115**, 14129–14136.
85 J. P. Cerón-Carrasco, A. Requena, C. Michaux, E. A. Perpète and D. Jacquemin, *Chem. Phys. Lett.*, 2009, **484**, 64–68.
86 A. Gelasco and S. J. Lippard, *Biochemistry*, 1998, **37**, 9230–9239.
87 L. G. Marzilli, J. S. Saad, Z. Kuklenyik, K. A. Keating and Y. Xu, *J. Am. Chem. Soc.*, 2001, **123**, 2764–2770.
88 A. Kumar, M. Sevilla and S. Suhai, *J. Phys. Chem. B*, 2008, **112**, 5189–5198.
89 A. Kumar and M. D. Sevilla, *J. Phys. Chem. B*, 2009, **113**, 11359–11361.

